

Supporting Information

Title: Targeted treatment of Multiple Myeloma with a radioiodinated small molecule radiopharmaceutical

*Ankita Shahi^{1#}, Gerald E. Weiss^{1#}, Saswati Bhattacharya², Dana C. Baiu³, Roberta Marino⁴,
Taner Pula⁵, Natalie S. Callander², Fotis Asimakopoulos^{2,6}, and Mario Otto¹*

Author's affiliations:

¹Department of Pediatrics, School of Medicine and Public Health, Carbone Cancer Center, University of Wisconsin, Madison, WI, USA

²Department of Medicine, Division of Hematology/Oncology, School of Medicine and Public Health, Carbone Cancer Center, University of Wisconsin, Madison, WI, USA

³Department of Medical Microbiology and Immunology, School of Medicine and Public Health University of Wisconsin, Madison, WI, USA

⁴Department of Therapeutics Production and Quality, St. Jude Children's Research Hospital, Memphis, TN, USA

⁵Department of Pediatrics and Adolescent Medicine, Ulm University Medical Center, Ulm, Germany

⁶Department of Medicine, Division of Blood and Marrow Transplantation, Moores Cancer Center, University of California-San Diego, La Jolla, CA, USA

#AS and GEW contributed equally to this work

Corresponding author: Mario Otto, Department of Pediatrics, School of Medicine and Public Health, Carbone Cancer Center, University of Wisconsin, Madison, WI, USA. Email:

motto@pediatrics.wisc.edu

1. Supplementary Material and Methods

Cell Lines and Primary Cells

The multiple myeloma (MM) cell line MM1.R was purchased from ATCC (Manassas, VA, USA). U-266 was purchased from Creative Biolabs (Shirley, NY, USA). MM1.S, RPMI8226, and KMS-12-BM were kindly provided by Dr. Fotis Asimakopoulos (University of Wisconsin-Madison). In our lab, the authenticity of cell lines obtained from non-commercial sources within 12 months of the start of experiments is routinely verified via genomic short tandem repeat profiling (UW-Madison Pathology Core Lab). We perform periodic PCR and HEK-Blue LPS testing (Invivogen, San Diego, CA, USA) to verify cell lines are free of bacterial contaminants, including Mycoplasma species. Peripheral blood was collected from healthy individuals on an IRB-approved protocol and peripheral blood mononuclear cells (PBMC) isolated by standard density gradient centrifugation with Lymphoprep, according to the manufacturer's instructions (Stem Cell Technologies, Cambridge, MA, USA). MM patient bone marrow aspirate samples were obtained under informed consent at the University of Wisconsin Hospital and Clinics, on IRB-approved research protocol HO07403 (PI: Callander).

Synthesis of CLR 127 and Its Radioiodinated, Fluorescent and Near-Infrared Analogs

CLR 127, fluorescently labeled CLR 127-BODIPY (CLR1501), the near-infrared emitting CLR 127-IR-775 (CLR1502) and its radioactive analogs CLR 124 and CLR 131 were kindly provided by Collectar Biosciences, Inc. (Florham Park, NJ, USA, previously Madison, WI, USA) and Dr. Jamey Weichert, University of Wisconsin-Madison. Methods for the synthesis of CLR 127, radioiodination, and purification and synthesis of CLR1501 and CLR 1502 have been previously

published (1). All radiopharmaceuticals for *in vivo* use were prepared under current good manufacturing practice (cGMP) guidelines.

CLR1501 and CLR1502 Uptake Experiments

CLR1501 uptake, serving as an *in vitro* surrogate for uptake of CLR 127 and radioiodinated derivatives, was assessed by flow cytometry using standard protocols. In brief, MM or peripheral blood mononuclear cells (5×10^5 / ml) were incubated with $5 \mu\text{M}$ of CLR1501 for 16 h and washed with 10% FBS containing cell media for 6 h. Cells were collected and re-suspended in 250 μl of FACS buffer (PBS containing 1% BSA), stained with DAPI (AnaSpec, Fremont, CA, USA), and data acquired on a MACSQuant flow cytometer (Miltenyi Biotec, Auburn, CA). All experiments were repeated three times.

MM patient samples from 5 patients were acquired at diagnosis based on International Myeloma Working Group (IMWG) criteria. The percent of plasma cells varied but by definition was over 10% (no cases of MGUS were included). To test CLR1501 uptake in MM patient bone marrow, samples collected from the posterior iliac crest were filtered through $40 \mu\text{m}$ sieves and mononuclear cells isolated by density gradient centrifugation. These unfractionated mononuclear cells were incubated with CLR1501 for 1 h and 18 h and identified by immunofluorescence staining using mouse anti-human antibodies specific for CD38, CD56, CD19, CD138 (BioLegend, San Diego, CA) and analyzed for CLR1501 uptake in MM cells versus the non-MM cell fraction. MM cells were defined as $\text{CD38}^+ \text{CD56}^+ \text{CD19}^{+/-} \text{CD138}^+$. The fluorescence was measured on an LSR II flow cytometer (BD, Franklin Lakes, NJ). Data analysis was performed using FlowJo software (BD Biosciences, San Jose, CA, USA) and the mean fluorescence intensity corrected for differences in cell size by normalizing to autofluorescence.

Uptake of CLR 127 in bone marrow MM cells (defined as CD138⁺ CD38⁺ CD56⁺ fraction) compared to bone marrow plasma cells (CD38⁺ CD138⁺ CD56⁻) and non-B cells (CD19⁻ CD38⁻ CD138⁻ CD56⁻) was determined using the near-infrared analog CLR1502 as surrogate, with the same sample preparation and data analysis as described above.

Data are presented as mean \pm standard error (bars). $P \leq 0.05$ was considered statistically significant. The unpaired two-tailed Student's *t*-test was used to analyze comparisons between individual groups where applicable.

In Vivo PET/CT Image Data Acquisition, Processing, and Analysis

PET/CT data acquisition and data analysis were performed as we have previously published (2). In brief, once tumor size reached a minimum of about 180 mm³, mice (n=4) were injected with 150 μ Ci of CLR 124 via tail-vein. After 96 hours, PET/CT image data were acquired under anesthesia on an Inveon micro-PET/CT scanner (Siemens, Knoxville, TN) in 3D acquisition mode. Static PET data acquisition was terminated once a minimum of 40 million counts were collected, followed by a CT scan without removing the animals from the scanner. PET images were reconstructed in 3D mode using the ordered-subset expectation maximization (OSEM3D) maximum *a posteriori* (MAP) algorithm. Regions of interest (ROI) were segmented for the tumors and muscle tissue based on axial slices of the CT data. Mean PET tracer uptake values and standard deviation of the CT-based ROIs were extracted using the *Material Statistics* module. Tumor-to-muscle-ratios (TMR) were calculated for each subject, by normalizing the tumor ROI uptake values to the mean uptake value of the muscle ROI.

Molecular-Targeted Radiotherapy with CLR 131 in MM1.S Flank Xenograft Models

All animal studies were performed under the approval of the University of Wisconsin Institutional Animal Care and Use Committee (IACUC) in compliance with National Institutes of Health (NIH) guidelines. 3×10^6 MM1.S tumor cells in 200 μ l PBS were injected subcutaneously into the left flank of NOD.Cg-Prkdc^{scid} Il2rg^{tm1Wjl}/SzJ (NSG) mice (Jackson Laboratory, Bar Harbor, ME, USA). Mice were randomized to either a control (n=13) or treatment cohort (n=14) when average tumor volumes reached approximately 500 mm³. Treatment mice were injected with a single dose of 3.7 MBq CLR 131 via lateral tail vein. Control mice were injected with an equal volume of excipient (vehicle only). All mice received 1 mg/20g body weight of potassium iodide intraperitoneally daily for 3 doses, starting the day prior to radionuclide injection, for thyroid blockade. Tumor growth was monitored twice weekly by direct measurement with calipers, and body weight was recorded. Tumor volume was calculated using the formula $[V = (\text{length} \times \text{width}^2)/2]$. The R version 3.5.1 software was used to generate the mixed linear effects model graph for the tumor growth rate and the Kaplan-Meier survival graph.

Hematotoxicity associated with radiotherapy was determined by collecting peripheral blood samples via maxillary sinus bleed from 4 mice immediately before and 7, 14, and 21 days after CLR 131 injection. Blood samples were collected into EDTA capillary tube and run on a VETScan HM5 hematology analyzer (Abaxis, Union City, CA) adjusted for mouse hematology analysis for the evaluation of total white blood cell count, lymphocytes, platelets, and hemoglobin. The unpaired two-tailed Student's *t*-test was used for statistical analysis. $P \leq 0.05$ was considered statistically significant.

Molecular-targeted Radiotherapy with CLR 131 in an MM1.S Orthotopic Bone Marrow Xenograft Model

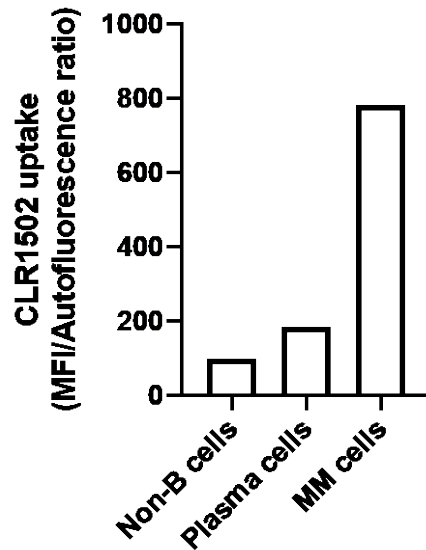
Orthotopic MM xenografts were established in NSG mice (n=5) by injecting 5×10^6 MM1.S cells (suspended in 150 μ L of PBS) into the lateral tail vein. Engraftment and disease progression were monitored by periodically measuring human lambda light chain levels as previously reported (3). Blood sampling was performed via tail vein nick. Human lambda light chain levels in mouse serum were quantified by ELISA using a commercial kit according to the manufacturer's instructions (Bethyl Laboratories, Montgomery, TX, USA). In brief, mice were randomized to treatment or control cohort when a lambda light chain concentration was detected in a range between 10-20 μ g/ml. Mice were injected with either a single, 3.3 MBq dose of CLR 131 or an equal volume of excipient. Blood was collected from each mouse via tail vein once weekly. Serum was obtained via centrifugation technique, collected, and stored at -20°C until the full radioactive decay of the radioactive samples was below radiosafety threshold. The ELISA was then performed on all treatment and control samples simultaneously. The unpaired two-tailed Student's *t*-test was used for statistical analysis. $P \leq 0.05$ was considered statistically significant.

2. Supplementary Figures

Supplementary Figure S1: Schematic representation of CLR 127 and analogs.

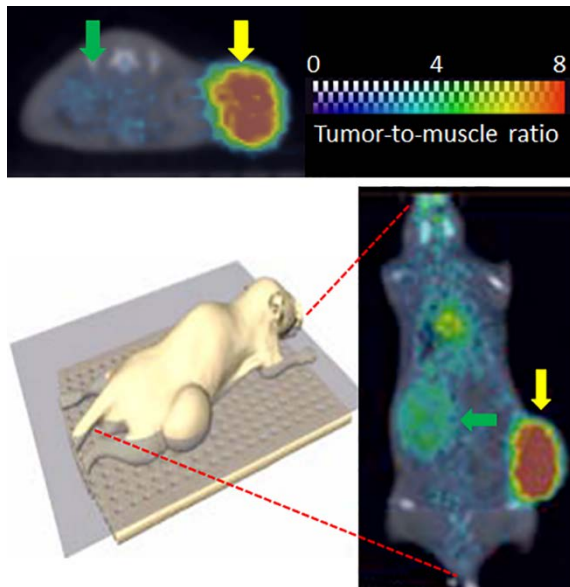
Supplementary Fig. S1: **Schematic representation of CLR 127 and analogs.** Chemical structure of the tumor-selective alkyl phosphocholine analog 18-(p-iodophenyl) octadecyl phosphocholine (CLR 127), its radioiodinated analogs (CLR 124 and 131), fluorescent BODIPY derivative (CLR1501), near-infrared emitting analog (CLR1502), and their applications.

Supplementary Figure S2: Uptake of CLR 1502 in bone marrow myeloma cells compared to bone marrow plasma and non-B cells



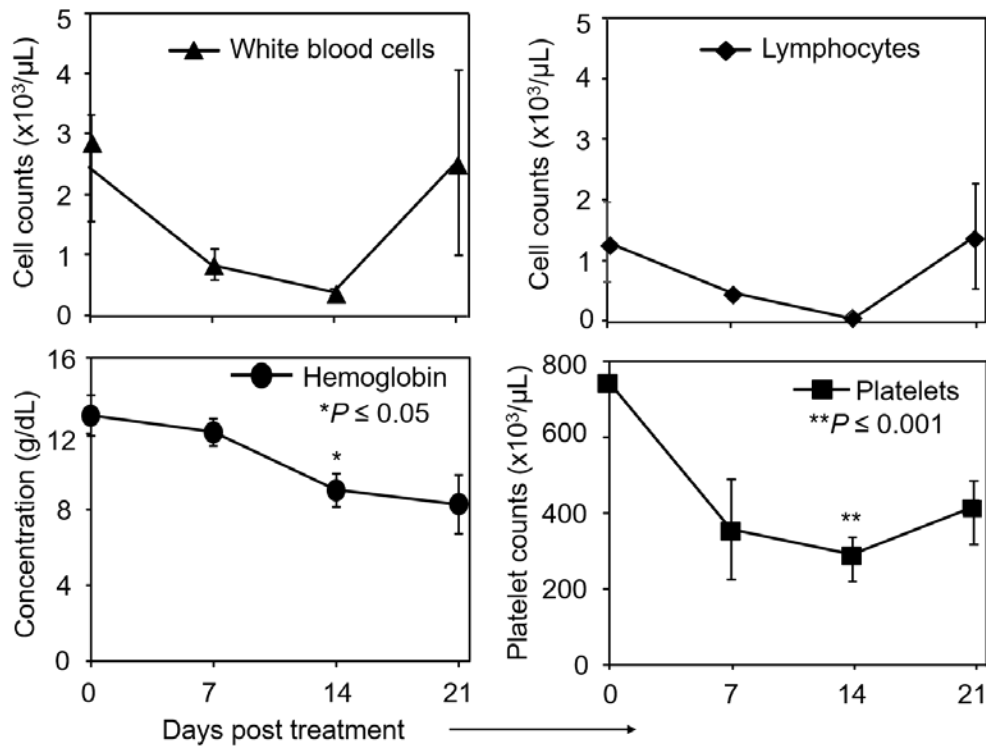
Supplementary Fig. S2: **Uptake of CLR 1502 in MM cells compared to plasma cells and non-B cells.** Flow cytometry analysis of an MM bone marrow sample of one patient, gated on non-B cells (CD19- CD38- CD138- CD56-), plasma cells (CD38+ CD138+ CD56-) and MM cells (CD38+ CD138+ CD56+) indicates a 4.2-fold higher uptake of CLR1502 in the MM cells when compared with plasma cells.

Supplementary Figure S3: Uptake of CLR 124 in a MM1.S flank xenograft model



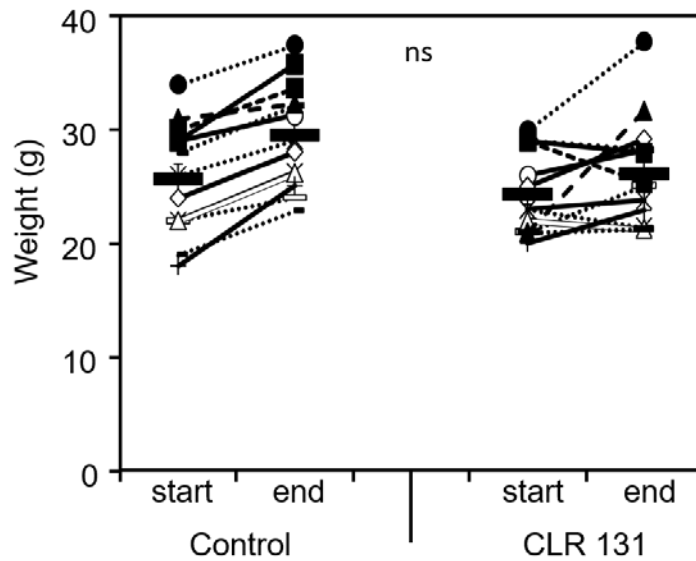
Supplementary Fig. S3: Uptake of CLR 124 in a MM1.S flank xenograft model illustrated by axial and coronal PET/CT orthoslices. *Upper panel:* Axial PET/CT orthoslice (i.e., section through CT data set with corresponding PET data ‘color-washed’ in) demonstrating selective tumor uptake (yellow arrow) and hepatic blood pool activity (green arrow). *Lower panel:* Coronal section through a PET/CT data set demonstrating CLR 124 uptake levels in tumor xenograft (yellow arrow), blood pool activity in the liver (green arrow) and heart at 96 hours post injection. Representative images of n = 3 scanned animals are shown.

Supplementary Figure S4: Effects of single-dose CLR 131 treatment on peripheral blood hematological parameters in tumor-bearing mice



Supplementary Fig. S4: **Assessment of hematotoxicity in MM1.S flank tumor bearing mice after treatment with a single dose (3.7 MBq) of CLR 131.** Complete blood count is shown compared to baseline values prior to CLR 131 injection in n=4 representative mice. Upper panels: Total leukocyte and lymphocyte counts decreased to day 14, and recovery documented by day 21. Lower panels: Hemoglobin concentration and platelet counts were found significantly decreased at day 14, with a nadir at day 21 (* $P \leq 0.05$; ** $P \leq 0.001$). Data points depict mean \pm standard error (vertical bars).

Supplementary Figure S5: Effects of single-dose CLR 131 treatment on animal weight



Supplementary Fig. S5: **Effects of single-dose CLR 131 treatment vs. vehicle on tumor-bearing mice.** Animal weight was recorded twice weekly. Lines depict weight development in mice that were injected with 3.7 mBq CLR 131 (n=14) or vehicle (control cohort, n=13). No weight loss or otherwise significant change in animal weight was observed in CLR 131 treated mice compared to the control cohort (ns = not significant).

References

1. Weichert JP, Clark PA, Kandela IK, et al. Alkylphosphocholine analogs for broad-spectrum cancer imaging and therapy. *Sci Transl Med.* 2014;6(240):240ra75.
2. Marino R, Baiu DC, Bhattacharya S, et al. Tumor-selective anti-cancer effects of the synthetic alkyl phosphocholine analog CLR1404 in neuroblastoma. *Am J Cancer Res.* 2015;5(11):3422-3345.
3. Jia D, Koonce NA, Halakatti R, et al. Repression of multiple myeloma growth and preservation of bone with combined radiotherapy and anti-angiogenic agent. *Radiat Res.* 2010;173(6):809-817.